Tribarium *tetrahedro*-Tetragermanide Acetylenide, Ba$_3$[Ge$_4$][C$_2$]: Synthesis, Structure, and Properties

Jan Curda, Wilder Carrillo-Cabrera, André Schmeding, Karl Peters, Mehmet Somer, and Hans Georg von Schnering*

Stuttgart, Max-Planck-Institut für Festkörperforschung

Professor Walter Siebert zum 60. Geburtstag gewidmet

Abstract. Ba$_3$Ge$_4$C$_2$ is formed at 1530 K from the elements or by reaction of BaC$_2$ with BaGe$_2$ (corundum crucible; steel ampoule). The compound is a semiconductor (grey colour; E$_g$ = 1.1 eV), brittle, very sensitive to moisture, and reacts with NH$_4$Cl at about 400 K forming acetylene and germanes up to Ge$_4$H$_n$. The new Ba$_3$Ge$_4$C$_2$ structure type (space group *I4/mcm*, No. 140; a = 8.840(1) Å, c = 12.466(1) Å; Z = 4, Pearson code *tI*36), contains two kinds of isolated polyanions, namely *tetrahedro*-tetragermanide [Ge$_4$]$^{4-}$ and acetylenide [C$_2$]$^{2-}$ anions. The bond lengths are d(Ge–Ge) = 2.517 Å (4×) and 2.641 Å (2×), and

d(C≡C) = 1.20 Å. The Ba$_3$[Ge$_4$][C$_2$] structure is a hierarchical derivative of the perovskite (CaTiO$_3$) generated by a partial atom/cluster replacement ([Ge$_4$] for Ca, [C$_2$] for Ti and Ba for O). The Raman spectrum shows bands at 168, 199 and 280 cm^{-1}, and at 1796 cm^{-1} characteristic for [Ge$_4$]$^{4-}$ and [C$_2$]$^{2-}$ polyanions, respectively.

Tribarium-*tetrahedro*-Tetragermanid-Acetylenid, Ba$_3$[Ge$_4$][C$_2$] – Synthese, Struktur und Eigenschaften

Inhaltsübersicht. Ba$_3$Ge$_4$C$_2$ bildet sich aus den Elementen oder durch die Umsetzung von BaC$_2$ mit BaGe$_2$ bei 1530 K (Korundtiegel in geschlossener Stahlampulle). Die Verbindung ist ein Halbleiter (grau; E$_g$ = 1.1 eV), spröde, und sehr feuchtigkeitsempfindlich. Sie reagiert mit NH$_4$Cl bei ca. 400 K unter Bildung von Acetylen und Germanen bis Ge$_4$H$_n$. Der neue Ba$_3$Ge$_4$C$_2$-Strukturtyp (Raumgruppe *I4/mcm*, No. 140; a = 8.840(1) Å, c = 12.466(1) Å; Z = 4, Pearsonsymbol *tI*36) enthält zwei isolierte Polyanionen, nämlich

Tetrahedro-tetragermanid [Ge$_4$]$^{4-}$ und Acetylenid [C$_2$]$^{2-}$. Die Bindungslängen betragen d(Ge–Ge) = 2.517 Å (4×) bzw. 2.641 Å (2×) und d(C≡C) = 1.20 Å. Die Struktur von Ba$_3$[Ge$_4$][C$_2$] ist durch Atom/Cluster-Substitutionen ([Ge$_4$] statt Ca; [C$_2$] statt Ti; Ba statt O) eine hierarchische Variante der Perowskit-Struktur CaTiO$_3$. Das Raman-Spektrum zeigt Banden bei 168, 199 und 280 cm^{-1} bzw. 1796 cm^{-1}, die für die Polyanionen [Ge$_4$]$^{4-}$ und [C$_2$]$^{2-}$ charakteristisch sind.

1 Introduction

It is well known that in the binary Ge–C system no compounds are formed, e. g. the SiC analogue. In order to explore ternary phases with Ge–C frameworks or

clusters, we studied some ternary systems (Ba–Ge–C, Ca–Ge–C, Li–Ge–C) and obtained the novel phase Ba$_3$Ge$_4$C$_2$ [1].

The full characterisation of this phase shows again that no heteroatomic Ge–C species are present but only homoatomic polyanions, namely *tetrahedro*-tetragermanide [Ge$_4$]$^{4-}$ and acetylenide [C$_2$]$^{2-}$ anions. In the present paper, the preparation, crystal structure, Raman and IR spectra, and some properties of the first germanide acetylenide Ba$_3$Ge$_4$C$_2$ are reported (the [C$_2$]$^{2-}$ anion is also called acetylide anion or dicarbide(2-)anion).

* Correspondence Address:

Prof. Dr. Dres. h. c. H. G. von Schnering
Max-Planck-Institut für Festkörperforschung
Heisenbergstr. 1
D-70569 Stuttgart

2 Synthesis

$Ba_3Ge_4C_2$ may be synthesised from the elements or by reaction of $BaGe_2$ with BaC_2. The starting materials as well as the products are sensitive to air and/or moisture, and were handled in an argon-filled glove box ($O_2 < 1$ ppm and $H_2O < 1$ ppm), which is equipped with a microscope. The barium metal used (3 N, Aldrich), was first distilled under high vacuum, the germanium (5 N, Preussag) and graphite (graphite rod 1.27×55 cm, Alpha) were used as purchased.

First method: $Ba_3Ge_4C_2$ is formed by reaction of $BaGe_2$ with BaC_2 (ratio 2/1) at 1530 K. The powders of the binary samples were mixed and filled in a corundum crucible, all together sealed in a stainless steel ampoule, heated at 1530 K for about 8 h and then cooled to room-temperature (50 K/h). The binary educts were prepared from stoichiometric mixtures of the elements, sealed in tantalum (BaC_2 case) or stainless steel ($BaGe_2$ case; inner corundum crucible) ampoules, and heated at different temperatures, BaC_2: 3 h at 1320 K followed by 6 h at 1170 K and then cooled to room-temperature (8 h). $BaGe_2$: 2 h at 1370 K, cooled first to 1070 K (12 h) and then to room-temperature (6 h).

Second method: $Ba_3Ge_4C_2$ may also be prepared from the elements as reactants. Barium, germanium and graphite (atomic ratios Ba/Ge/C = 3/4/2) are filled in an inner corundum crucible, sealed in a stainless steel ampoule and heated at 1530 K for 8 h, followed by cooling to room-temperature (50 K/h). X-ray powder patterns show that the elements react first to the binary phases $BaGe_2$ and BaC_2 (at $T \approx 1200$ K), and, therefore, the synthesis from the elements is in principle the same as the first method described above.

In order to get high yields, the sample must be heated for a second time (after grinding and mixing) in both procedures. Typical batch sizes were 1.5–2.5 g. The sealed stainless steel ampoules used for the reactions have diameter $\phi = 16$ mm and length $l \approx 80$ mm.

The X-ray powder diffraction patterns (Stoe diffractometer, $CuK\alpha_1$ radiation) of the samples prepared at 1530 K showed only reflections of $Ba_3Ge_4C_2$. However, minor amounts of amorphous carbon might be still present in the samples, which is indicated by a broad band observed in the corresponding Raman spectrum (Fig. 2). In samples prepared by direct synthesis at temperatures below 1300 K no ternary phase was formed. Only $BaGe_2$ and BaC_2 were observed by X-ray powder diffraction.

3 Properties

The compound is grey, brittle and very sensitive to moisture. It decomposes rapidly in wet air to an unknown product of yellowish orange colour, which appears to be amorphous. In samples exposed to dry oxygen or nitrogen no reaction was observed at temperatures lower than 375 K. $Ba_3Ge_4C_2$ reacts rapidly with water and mineral acids forming acetylene gas and Ge_mH_n (see section 4). Thermogravimetric measurements (297–1000 K) in high-vacuum show that $Ba_3Ge_4C_2$ is very stable at temperatures below 1000 K. DTA measurements of a $Ba_3Ge_4C_2$ sample in a corundum crucible and argon atmosphere (heating/cooling rate = 20 K/min, $T_{max} = 1650$ K) show two endothermic peaks during heating as well as cooling, which indicates an incongruent melting with a peritectic reaction at 1340 K and a total melting at 1520 K.

The optical band gap of $Ba_3Ge_4C_2$ is 1.1 eV as determined by diffuse reflection. This value is in agreement with the observed grey colour. For the optical diffuse reflection experiment (data recorded with a Perkin Elmer Lambda 9 spectrometer), a powdered $Ba_3Ge_4C_2$ sample was first diluted with MgO powder and then filled in a sealed silica tube.

4 Protolytic reactions of $Ba_3Ge_4C_2$

The X-ray structure analysis (see section 5 and Ref. [1]) has shown that this new compound contains *tetra-hedro*-tetragermanide $[Ge_4]^{4-}$ and very probably acetylenide $[C_2]^{2-}$ anions. In order to proof chemically that $Ba_3Ge_4C_2$ really contains the acetylenide anion, several experiments were carried out. The main aim was to produce acetylene by the reaction of $Ba_3Ge_4C_2$ with different protolytes: (a) H_2O, (b) $KHSO_4$ (dried at 390 K in vacuum) and (c) NH_4Cl (dried at 370 K). The experiments (b) and (c) were achieved under similar conditions in an evacuated thermo-balance equipped with a mass-spectrometer. The formation of acetylene was observed in each case, and reaction (c) also shows the formation of a series of germanes.

Previously to experiment (b), the formation of acetylene by the reaction of BaC_2 with $KHSO_4$ (ratio 1:4) was carried out successfully.

4.1 Protolysis with H_2O

The reaction of $Ba_3Ge_4C_2$ with water was performed in an arrangement analogue to the Marsh's test for arsenic, but under inert conditions (O_2-free water, Ar atmosphere). At room temperature, the reaction is rather slowly (only few bubbles are recognised). When the mixture is heated the reaction becomes violent. The liberated gas burns with fuliginous flame, which is characteristic for acetylene. No metal mirror (Ge) could be observed when the glass capillary was locally heated, indicating that no volatile germanes were formed under the given conditions. The reaction yielded an amorphous brownish-red residue which was not characterised. It should be notice that this is the more simple and cheaper experiment of all three.

4.2 Protolysis with KHSO$_4$

As mentioned before, the reaction of Ba$_3$Ge$_4$C$_2$ with KHSO$_4$ (ratio 1:2) was performed in an evacuated thermo-balance equipped with a mass-spectrometer. Acetylene was produced in the range 340–630 K with two maxima at about 420 and 610 K. In the mass-spectrum, besides the signals for H$_2$, H$_2$O (maximum at 460 K) and acetylene (m/e = 26), other weaker signals (m/e = 25, 24, 13) characteristic for the fragmentation of C$_2$H$_2$ were also observed. Furthermore, another signal verified the production of GeH$_n$ (maximum at 510 K; [m/e]$_{max}$ = 77).

In this experiment the first reaction liberating C$_2$H$_2$ (maximum at 420 K) seems to be stopped at about 450 K due to the formation of a passivation layer of BaSO$_4$ on the surface of the Ba$_3$Ge$_4$C$_2$ particles. Therefore, between 450 and 580 K only the simple thermal decomposition of KHSO$_4$ take place (forming H$_2$O and K$_2$SO$_4$). At higher temperature, the passivation layer crushes and the reaction starts again, liberating C$_2$H$_2$ and some GeH$_n$.

4.3 Protolysis with NH$_4$Cl

The reaction with NH$_4$Cl was planed in order to avoid the problems which occur with KHSO$_4$. Indeed, this reaction take place without difficulties, but quite unexpected, it shows the transformation of the tetrahedro-tetragermanide anion into several polygermanes, maintaining the homoatomic Ge–Ge bonds.

The reaction of Ba$_3$Ge$_4$C$_2$ with NH$_4$Cl (ratio 1:6) was carried out similarly to that described in section 4.2. In this case, acetylene and H$_2$ was formed in the range 330–440 K. As shown in the mass-spectrum recorded at T = 410 K (Fig. 1), acetylene and a series of germanes Ge$_m$H$_n^+$ (m = 1–4; n = 2 m + 1) were the
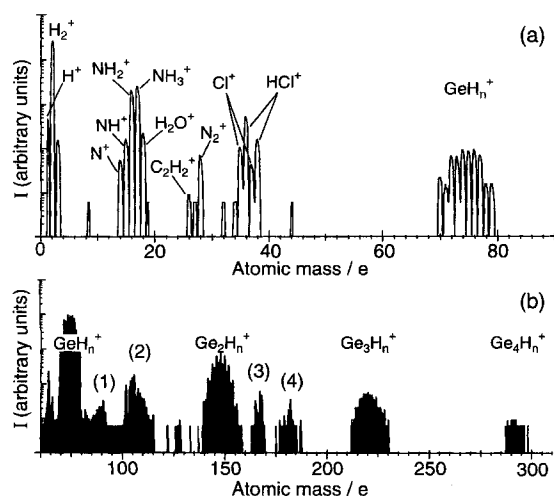
Fig. 1 Mass spectrum of the gaseous products of the reaction of Ba$_3$Ge$_4$C$_2$ with NH$_4$Cl at T = 410 K. (a) $0 \leq$ m/e ≤ 90 (atomic mass)/e range. (b) $60 \leq$ m/e ≤ 310.

main gaseous products of the reaction together with NH$_3$, HCl and their fragments. In Fig. 1, the signals indicated by (2) and (4) ([m/e]$_{max} \approx 108$, 182) can be assigned to the fragments of some chloro-germanes Ge$_m$H$_p$Cl$_{4-p}$. The weaker signals indicated by (1) and (3) in Fig. 1 ([m/e]$_{max} \approx 90$, 166) might be originated from gaseous species containing Ge and N (or O).

5 Structure Determination and Refinement

Single crystals of the title compound were isolated and sealed in glass capillaries. The quality of the crystals was controlled by the film methods. The X-ray diffraction data were measured on a Siemens P4 four-circle diffractometer. The Laue symmetry and the systematic reflection absences are consistent with the space-groups *I4/mcm* (No. 140) and *I422* (No. 97). The centrosymmetric alternative was chosen and finally confirmed in the refinement. The unit cell dimensions were determined from the least-squares refinement of the 2θ values of 67 reflections ($11.3° < 2\theta < 24.6°$). The crystallographic data are presented in Table 1.

The exact chemical composition of the crystals from the Ba–Ge–C samples was not known during the crystal structure determination. From a series of systematic studies carried out in order to vary the structure of the clathrates M$_x$(X,Y)$_{46}$, M$_x$(X,Y)$_{136}$ and M$_x$(X,Y)$_{25}$ with M = alkaline metal, earth alkaline metal and X,Y = E14, E13 elements or M = halogen and X,Y = E14, E15 elements, and from studies of the tetrahedrane derivatives with [X$_4$]$^{4-}$ (X = E14) [3], we know about the formation of byproducts like Ba$_{10}$Ge$_7$O$_3$ [4], as a result of reactions with the corundum crucible. Therefore, the possibility that the new phase contained oxygen was also considered.

Direct methods were used to solve the crystal structure. 59 unique reflections with $|E| > 1.5$ were included in the sign determination. The E map of the best solution yielded the location of two barium atoms (4a and 8h sites) and one germanium atom (16l site). Inside a Ba$_6$ octahedral cavity (centred at 4b 000) a significant electron density rest was revealed through difference Fourier syntheses. The electron density corresponds approximately to that of an oxygen atom, and an O^{2-} anion would fit the electron balance of a Zintl phase: (Ba^{2+})$_3$(Ge$_4$)$^{4-}$ O^{2-}. However, a very large displacement parameter $U_{iso} = 2100$ pm^2 results with an oxygen atom at 4b ($R(F) = 0.038$), indicating a much smaller scattering length or a strong anisotropy ($U_{11} = U_{22} = 1945$ pm^2, $U_{22} = 449$ pm^2). More accurate difference Fourier syntheses showed that the 4b peak position was split into four positions of a 16k site. The refinement showed then that the total scattering length f(X) is in the range $1.3 \times$ f(O) < f(X) < $1.4 \times$ f(O), which is close to the scattering length of two carbon atoms. The distance between two diagonal points of the four split positions is about 1.2 Å, which

is really a d(C≡C) bond length. At this stage, we were sure that the compound was a germanide *acetylide*, which also fits the electron balance with $[C_2]^{2-}$. Moreover, the Ba_6 octahedral cavity is slightly compressed

Table 1 Crystallographic data

Formula; Mole mass	$Ba_3Ge_4C_2$; 726.40 amu
Crystal characteristics	grey lump, $0.15 \times 0.12 \times 0.10$ mm
Space group; formula units	*I4/mcm* (No. 140); Z = 4
Structure type; Pearson code	$Ba_3Ge_4C_2$; *tI* 36
Unit cell dimensions (297 K)	$a = 8.840(1)$ Å, $c = 12.466(1)$ Å $c/a = 1.410$; $V = 974.2(2)$ Å^3
d_{calc}	4.953 g · cm^{-3}
Measurement (297 K)	Siemens P4 four-circle diffractometer, MoKα ($\lambda = 0.71073$ Å); ω-scan mode; $2\theta \leq 55°$
Data correction	empirical absorption correction (ψ-scan), $\mu = 239$ cm^{-1}, transmission: 0.05 to 0.14.
Structure determination	SHELXTL [2]; 15 variable parameters, $w = [\sigma(F_o)]^{-2}$
Measured/unique N(hkl)	800/325
N'(hkl) $[F_o > 3 \cdot \sigma(F_o)]$	292
$R(F)$; $R_w(F)$	0.033; 0.033

along [001], resulting in two shorter (3.116 Å) and four longer (3.246 Å) Ba-(4 b) distances, and also this feature fits much better with an orientational disordered dumbbell oriented in two perpendicular directions (black or white in Fig. 5b) around 4 b in the Ba_6 octahedral cavity.

The refinement of the heavy atoms ($R(F) = 0.033$, 16 refined parameters) resulted in an elongated displacement ellipsoid for the Ba2 at 8 h position (Table 2), which build up the octahedral coordination polyhedron around the orientational disordered C_2 units, as shown in Fig. 5 b. This feature is obviously correlated with the orientational disorder of the C_2 dumbbells. The final refinement with split positions (Ba2 at two 16 b sites around 8 h with occupancy 0.50 and about 0.36 Å apart) resulted in normal isotropic displacement parameters and a more reasonable elongated octahedral environment for the C_2 dumbbell (Fig. 5 c and Table 2; final $R(F) = 0.033$, 15 refined parameters).

The final atomic parameters are presented in Table 2. The main interatomic distances and bond angles are given in Table 3. The positional and displacement parameters for a model with Ba2$_{av}$ at 8 h position (no splitting) has been published elsewhere [1]. Additional material can be ordered re-

Table 2 Positional and displacement parameters (pm^2) for $Ba_3Ge_4C_2$. Space group *I4/mcm*, No. 140. The displacement factor is of the form: $\exp[-2\pi^2 (U_{11}h^2a^{*2} + \ldots + 2 U_{23}klb^*c^*)]$. Standard deviations are given in parentheses. The average position Ba2$_{av}$ is listed at the bottom.

Atom	Site	SOF	x	y	z	U_{11}/U_{iso}	U_{22}	U_{33}	U_{12}	U_{13}	U_{23}
Ba1	4 a	1	0	0	1/4	208(4)	U_{11}	228(6)	0	0	0
Ba2 [a]	16 k	0.5	0.1943(1)	0.6654(1)	0	189(4)					
Ge	16 l	1	0.10567(8)	x + 1/2	0.31772(9)	214(4)	U_{11}	191(6)	–34(4)	–35(2)	U_{13}
C [b]	16 k	0.5	0.058(3)	0.035(3)	0	368(55)					
[Ba2$_{av}$	8 h	1	0.17983(7)	x + 1/2	0	372(11)	U_{11}	215(5)	–217(4)	0	0]

[a]) Split position around 8 h x x + 1/2 0 with x = 0.1798 (±0.0145)
[b]) Split position around 4 b 0 0 0

Table 3 Main interatomic distances (Å) and bond angles (°) in $Ba_3Ge_4C_2$. The distorted Ba_6 octahedron in Fig. 5 c (with black Ba2 and Ba2' atoms) is assumed to be the ordered coordination polyhedron around the black C_2 dumbbell.

Ba1–C	3.174(5)	4×	Ge–Ge	2.518(2)	2×	Ge–Ba2$_{ave}$	3.458(1)	2×
–Ge	3.706(1)	8×	–Ge	2.642(2)		–Ba2$_{ave}$	3.515(1)	
			–Ba2	3.394(1)		–Ba2$_{ave}$	4.068(1)	
Ba2–C	2.82(3)		–Ba2'	3.520(1)				
–C	3.10(3)		–Ba2	3.532(1)		C–Ba2$_{ave}$	2.64(3)	
–C	3.16(3)		–Ba1	3.706(1)	2×	–Ba2$_{ave}$	3.30(3)	
–Ge	3.394(1)	2×				–Ba2$_{ave}$	3.31(3)	
–Ge	3.520(1)	2×						
–Ge	3.532(1)	2×	C–C	1.20(6)				
–Ge	4.072(1)	2×	–Ba2	2.82(3)				
			–Ba2'	3.10(3)				
∡ Ge–Ge–Ge	58.36(2)°	8×	–Ba2'	3.16(3)				
∡ Ge–Ge–Ge	63.28(5)°	4×	–Ba1	3.174(5)	2×			

ferring to the Nos. CSD-402340 and CSD-406662, names of the authors and title of the paper at the Fachinformations-zentrum Karlsruhe, Gesellschaft für wissenschaftlich-technische Information mbH, D-76344 Eggenstein-Leopoldshafen, Germany.

6 Raman and IR measurements

The room temperature Raman spectrum was recorded from powdered Ba$_3$Ge$_4$C$_2$ samples (sealed in silica tube) with a module FRA 106 (Nd: YAG-Laser, 1.064 nm, 200 mW) attached to a Bruker IFS 66v spectrometer. The infrared transmission spectrum was obtained from Ba$_3$Ge$_4$C$_2$–PE pellets with a Bruker IFS 113v spectrometer. The results are illustrated in
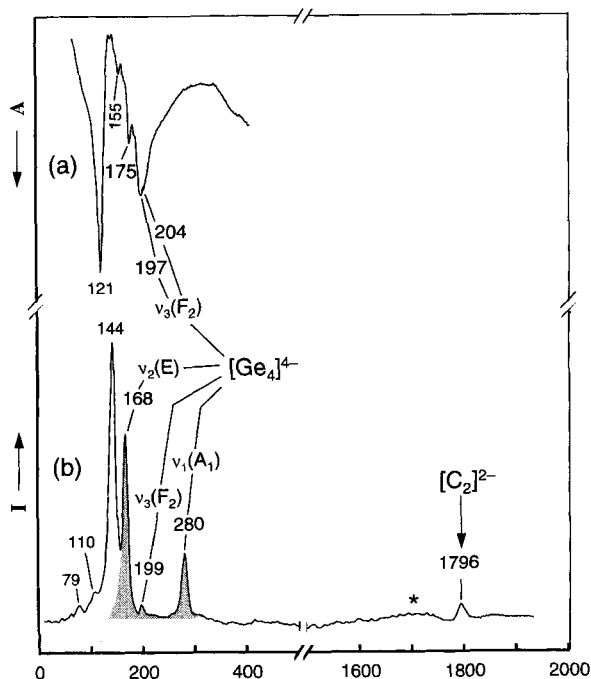
Fig. 2 (a) Raman and (b) infrared spectra of Ba$_3$Ge$_4$C$_2$ at room temperature. The frequencies of the bands are indicated (Table 4). *Due to amorphous carbon.

Table 4 Vibrational frequencies (cm^{-1}) of Ba$_3$Ge$_4$C$_2$ with assignement and relative intensities. The fundamentals of [Ge$_4$]$^{4-}$ in K$_7$LiGe$_8$ [10] are also listed.

Ba$_3$Ge$_4$C$_2$		Assignment	[Ge$_4$]$^{4-}$ [Ref.10]
R: 79 w, 110 w, 144 vs IR: 121 vs, 155 w		lattice modes	
R	IR		
175 w	168 vs	ν_2(E), [Ge$_4$]$^{4-}$	162
197 vs	199 w	ν_3(F$_2$), [Ge$_4$]$^{4-}$	200
204 sh	–		
280 ms	–	ν_1(A$_1$), [Ge$_4$]$^{4-}$	279
1796 mw	–	ν (C≡C), [C$_2$]$^{2-}$	

m = medium, v = very, s = strong, w = weak, sh = shoulder

Fig. 2, and the vibrational frequencies and intensities, as well as the proposed assignment, are summarised in Table 4. The Raman spectrum of BaC$_2$ was also recorded in a similar manner and, as expected, the characteristic frequency for [C$_2$]$^{2-}$ was observed in the high frequency region (ν(C≡C) = 1801 cm^{-1}).

7 Discussion

7.1 General

The semiconducting (E = 1.1 eV) ternary compound Ba$_3$Ge$_4$C$_2$ belongs to the Zintl phases because of the formation of polyanions, and according to the Zintl-Klemm concept [5, 6], its ionic formula is (Ba^{2+})$_3$[Ge$_4$]$^{4-}$[C$_2$]$^{2-}$. The vibrational spectra confirm completely the crystal structure with respect to the presence of quasi-isolated Ge$_4$ and C$_2$ units. At least, the chemical reactions with acids verify that Ba$_3$Ge$_4$C$_2$ contains the [C$_2$]$^{2-}$ and [Ge$_4$]$^{4-}$ anions. Here, the formation of acetylene was hopefully expected, but the preservation of large Ge$_m$H$_n$$^+$ fragments, up to Ge$_4$H$_n$$^+$, from solid Zintl phases was observed for the first time. It seems that this type of electrophilic reactions (e. g. with quaternary ammonium cations) may open a successful strategy to transform even larger Zintl anions into molecules.

It should be pointed out how easy Ba$_3$Ge$_4$C$_2$ is formed from the elements or better from the binary components BaGe$_2$ and BaC$_2$, and even from the melt (1520 K) in a peritectic reaction at about 1340 K. Again, there is no reaction of Ge with C to form Ge–C bonds. On the contrary, Ba$_3$Ge$_4$C$_2$ is simply a quasi-binary phase of the compounds BaGe$_2$ (with Ge$_4$ tetrahedra) and BaC$_2$ (with C$_2$ dumbbells). The reaction (Ge$_4$)Ba$_2$ + (C$_2$)Ba = (Ge$_4$)(C$_2$)Ba$_3$ is a direct analogue to the reaction of a Lewis base with a Lewis acid, e. g. TiO$_2$ + CaO = CaTiO$_3$ (perovskite; see section 7.2). On the other hand, it is delightful to see these two polyanions side by side, having the same oxidation state per atom and representing the preference of carbon to the monomere and of germanium to the dimere of a triply bonded X≡X unit.

7.2 Crystal structure

The compound Ba$_3$Ge$_4$C$_2$ forms a new structure type (*tI*36) which is a hierarchical cluster replacement derivative of the perovskite CaTiO$_3$:
CaTiO$_3$ $\overset{\triangle}{=}$ [Ge$_4$][C$_2$]Ba$_3$. The structure is characterised by acetylenide [C$_2$]$^{2-}$ and tetrahedro-tetragermanide [Ge$_4$]$^{4-}$ anions, which are nested in the octahedral and cuboctahedral cages, respectively, formed by the Ba^{2+} cations (Figs. 3–5).
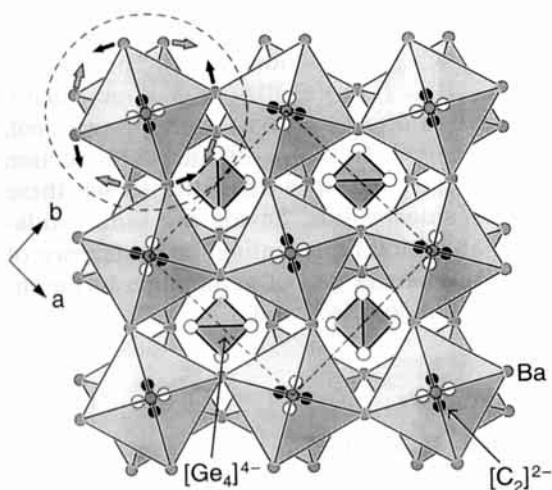
The acetylenide [C$_2$]$^{2-}$ anion has a bond length of d(C≡C) = 1.20(6) Å, close to that for [C$_2$]$^{2-}$ in the tetragonal CaC$_2$ (1.19 Å) [7]. The C$_2$ dumbbells in

$Ba_3Ge_4C_2$ are orientational disordered parallel to the basal plane along two of the (pseudo) 4-fold rotation axes of the barium octahedra (black or white in Fig. 5b).
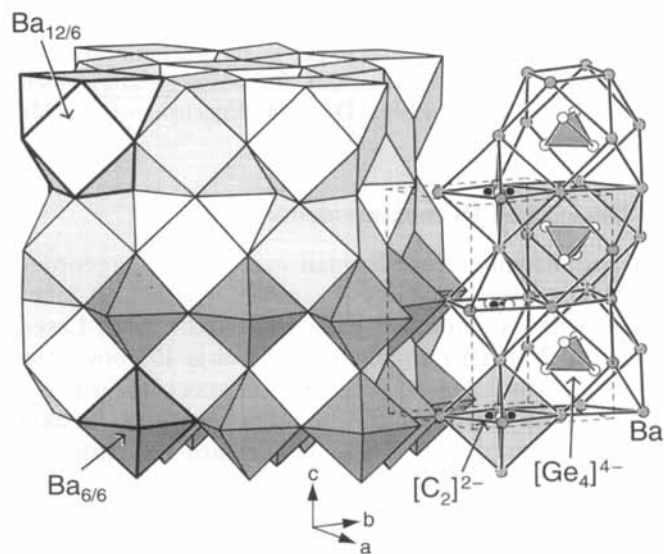
The tetrahedro-tetragermanide $[Ge_4]^{4-}$ anion is slightly compressed along the $\bar{4}$ axis, with bond lengths of $d(Ge-Ge) = 2.518(2)$ Å ($4\times$) and $2.642(2)$ Å ($2\times$), and bond angles of $58.36°$ and $63.28°$. Similar distortions have also been observed for one of the two types of Ge_4 tetrahedra in the alkaline metal monogermanides E1Ge (E1 = K, Rb, Cs) [3 g]. The mean value $\bar{d}$ (Ge-Ge) = 2.556 Å is 0.12 Å larger than the Ge-Ge single bond length. This agrees with the general observation in compounds with homonuclear polyanions [8]. Each Ge atom of a Ge_4 tetrahedron has five Ba next-neighbours (d(Ge-Ba) = 3.394 Å–3.706 Å; see Table 3) and one Ba2 atoms at a much longer distance (4.072 Å).

The crystal structure of $Ba_3Ge_4C_2$ can be described as a $^3_\infty[Ba_{6/2}]$ framework of twisted octahedra forming cuboctahedral cages, which can be derived from the regular $^3_\infty[O_{6/2}]$ framework of the perovskite structure (Fig. 3). The insertion of the Ge_4 tetrahedra causes a tetrahedral deformation of the Ba_{12} cuboctahedra (Figs. 4, 5 a) and the rotation of the Ba_6 octahedra, alternately clockwise and anti-clockwise around [001], as illustrated in Fig. 3.

As shown in section 5, a more detailed analysis of the barium arrangement indicates that the site of the Ba2 atoms is slightly split. But, for simplicity the average position $Ba2_{av}$ (Table 2) was used for most of the
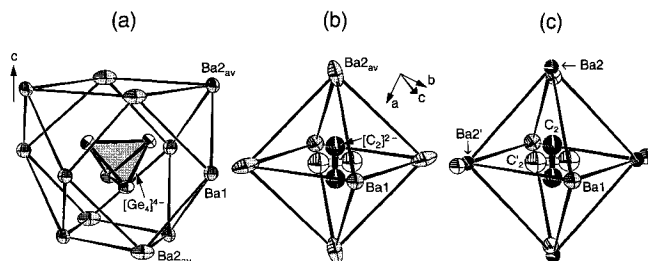

Fig. 4   The perspective view illustrates the space-filling arrangement of $Ba_{6/6}$ octahedra (centred by C_2) and distorted $Ba_{12/6}$ cuboctahedra (centred by Ge_4) in the $Ba_3Ge_4C_2$ structure.

figures presented here. The splitting means that at the short-range scale, the Ba2 atoms accommodate to a given orientation of the $[C_2]^{2-}$ anion, as shown in Fig. 5c. In an ordered model, each C_2 dumbbell cause then an elongation of its octahedral environment along one of the (pseudo) 4-fold rotation axes, which is parallel to the axis of the C_2 dumbbell. The d(C–Ba) distances split in two groups, one shorter along the axis of the C_2 dumbbell and four longer distances: 2.82 Å, 3.15 Å ($4\times$, average; Table 3). Thus, in the ordered domains, the cationic environment and the distribution of the d(C–Ba) distances for C_2 in $Ba_3Ge_4C_2$ are similar to those for C_2 in CaC_2 with

Fig. 3   Projection of the $Ba_3Ge_4C_2$ structure along [001]. The octahedral $^3_\infty Ba_{6/2}$ framework corresponds to the $^3_\infty O_{6/2}$ framework of the perovskite. The Ba_6 octahedra are centred by orientational disordered C_2 dumbbells (black/white), and the large cuboctahedral cavities are centred by the Ge_4 tetrahedra. Caused by the two perpendicular orientations of these tetrahedra in the basal plane, the Ba_6 octahedra are turned clockwise and anti-clockwise from layer to layer along [001] (arrows in the dashed circle; see text).

Fig. 5   The cavities of the Ba framework centred by the polyanions in $Ba_3Ge_4C_2$. (a) The tetrahedrally distorted cuboctahedron around the tetragermano-tetrahedrane $[Ge_4]^{4-}$ anion. (b) The octahedral environment around the acetylenide $[C_2]^{2-}$ anion. The pronounced elongation of the displacement ellipsoid of $Ba2_{av}$ is obviously correlated with the orientational disorder of the C_2 dumbbells (black or white). (c) Same as (b) but showing the splitting of $Ba2_{av}$ into two Ba2 with 50% probability. For the black C_2 dumbbell a possible ordering model for Ba2 (black Ba2 and Ba2′) is illustrated. The Ba octahedron is then elongated along the axis of the dumbbell. ORTEP plots with 75% probability.

d(C–Ca) = 2.595 Å and 2.814 (4×). Focusing the Ba2 atoms in the basal plane, the d(Ba2–C) *end-on* distance is 2.82 Å and the two *side-on* distances are 3.10 Å and 3.16 Å (Table 3).

As pointed out above, the Ba$_3$Ge$_4$C$_2$ structure is a hierarchical cluster-replacement derivative of the perovskite CaTiO$_3$, in which the cuboctahedral and octahedral cages formed by O atoms are centred by Ca and Ti, respectively. In order to get the Ba$_3$Ge$_4$C$_2$ structure from the perovskite, the Ca and the Ti atoms are replaced by Ge$_4$ tetrahedra and C$_2$ dumbbells, respectively (Figs. 3 and 4). The structures of Ba$_3$[SiO$_4$][O] and CaTiO$_3$ are also related in a similar way: CaTiO$_3 \stackrel{\wedge}{=}$ [SiO$_4$][O]Ba$_3 \stackrel{\wedge}{=}$ [Ge$_4$][C$_2$]Ba$_3$.

7.3 Vibrational Spectra

The Raman and IR spectra of Ba$_3$Ge$_4$C$_2$ are illustrated in Fig. 2, and the vibrational frequencies, intensities and proposed assignment are summarised in Table 4.

The spectroscopically relevant units of Ba$_3$Ge$_4$C$_2$ are the polyanions [C$_2$]$^{2-}$ with $D_{\infty h}$ symmetry and [Ge$_4$]$^{4-}$ with T_d symmetry. The C$_2$ dumbbell is expected to give raise to only one Raman-active vibration Σ_g. The six fundamentals of the isolated tetrahedrane anion [Ge$_4$]$^{4-}$ belong to the symmetry species:

$$\Gamma_{vib}\ (T_d) = A_1(R) + E(R) + F_2(R,\ IR),$$

with A$_1$ and E being only Raman-active, and F$_2$ both Raman- and IR-active.

In the crystal, the centre of each [Ge$_4$] tetrahedron occupy the lower symmetry site 4-S_4. The site symmetry analysis predicts that the A$_1$ mode of the "isolated" [Ge$_4$]$^{4-}$ ion remains as a singlet, while both the E and F$_2$ modes should split into doublets, and therefore a total of five Raman and three IR allowed bands are expected: $T_d \rightarrow S_4$: A$_1 \rightarrow$ A(R),
E $\rightarrow$ A(R) + B(R, IR), F$_2 \rightarrow$ B(R, IR) + E(R, IR).

According to the spectroscopic data of K$_4$Ge$_4$ [9] and K$_7$LiGe$_8$ [10] and the present measurement on BaC$_2$ (section 2.1), the room-temperature Raman spectrum of Ba$_3$Ge$_4$C$_2$ may be separated in three regions (Fig. 4):

 I. The external modes with v <150 cm^{-1}
 II. The fundamentals of the [Ge$_4$]$^{4-}$ anion with 160 < v < 300 cm^{-1}
 III. The C≡C stretch with v > 1700 cm^{-1}.

In the high-frequency region of the Raman spectrum a medium weak band is observed at 1796 cm^{-1}, assigned to the C≡C stretch mode, according to the value obtained for BaC$_2$ (v(C≡C) = 1801 cm^{-1}, section 2.1). The broadening of this band in Ba$_3$Ge$_4$C$_2$ might be correlated to the orientational disorder of the acetylenide anions.

Three of the predicted five Raman modes for

[Ge$_4$]$^{4-}$ are observed at 168 cm^{-1} (E, v_2), 199 cm^{-1} (F$_2$, v_3) and 280 cm^{-1} (A$_1$, v_1), in excellent agreement with those reported by *Kliche* et al. [10] for [Ge$_4$]$^{4-}$ in K$_7$LiGe$_8$: 162 cm^{-1} (E), 200 cm^{-1} (F$_2$) and 279 cm^{-1} (A$_1$). Nevertheless, the intensity of the F$_2$ Raman vibration is comparatively weaker in Ba$_3$Ge$_4$C$_2$, which may be a consequence of the different cationic environments of the tetrahedrane anions in both structures. A similar behaviour has also been observed for the Raman active fundamentals of the [Si$_4$]$^{4-}$ anion in the series M$_4$Si$_4$ (M = E1) [11], revealing a change in the intensity of the internal modes in correlation with the cationic environments and the type of the cations, whereas the positions of the characteristic frequencies remain almost unchanged.

The IR spectrum of Ba$_3$Ge$_4$C$_2$ exhibits in the frequency range 80–400 cm^{-1} a strong doublet, at 197 and 204 cm^{-1}, and a weak band at 175 cm^{-1} corresponding to the IR active components of the fundamentals F$_2$ and E, respectively. The weak splitting of the degenerated modes E and F$_2$ reveals that the deviation from the regular tetrahedrane is very small. Accordingly, the assignment of the observed frequencies given in Fig. 2 and Table 4 are based on the T_d symmetry of the "free" anion [Ge$_4$]$^{4-}$, taking into account the symmetry reduction to S_4.

The valence force constant f$_d$ and the interaction force constants f$_{dd}$ and f$_{dd}$ for [Ge$_4$]$^{4-}$ were calculated using the measured frequencies listed in Table 4 (the frequencies of the split modes E and F$_2$ were averaged): f$_d$ = 0.97 Ncm^{-1}, f$_{dd}$ = –0.06 Ncm^{-1} and f$_{dd}$ = 0.12 Ncm^{-1}. These values agree well with those previously reported [9, 10] and will not be discussed here.

However, of particular interest is the value of f(C≡C), the stretching force constant of the acetylenide anion [C≡C]$^{2-}$, for which no experimental data has been available yet. The observed frequency v(C≡C) = 1796 cm^{-1} (Table 4) results in a valence force constant of f(C≡C) = 11.41 Ncm^{-1}, which is very similar the that for [C≡C]$^{2-}$ in BaC$_2$ (11.47 Ncm^{-1}). Both values are considerably smaller than those reported for C$_2$H$_2$ and [C$_2$H]$^-$ [12, 13]: f(C≡C) = 15.74 and 13.05 Ncm^{-1}, respectively. The significant decrease in the (C≡C) valence force constants for the anions is consistent with the findings for CH$_2$=C=CH$_2$ and [C=C=C]$^{4-}$ [14, 15] with f(C=C) = 9.60 and 7.96 Ncm^{-1}, respectively, according to which an increase in anionic charge weakens the bonds, and in consequence reduces the frequencies and force constants. This is also in accordance with the observed changes in bond lengths in previous studies [8].

References

[1] H. G. von Schnering, J. Curda, W. Carrillo-Cabrera, M. Somer, K. Peters, *Z. Kristallogr.* **1996**, *211*, 634.

[2] G. M. Sheldrick, SHELXTL PLUS, *Realease 4.0 Programs for Solving, Refining and Displaying Crystal Structures*, Siemens Analytical X-Ray Instruments, 1990.

[3] a) H. Menke, H. G. von Schnering, *Z. Anorg. Allg. Chem.* **1973**, *395*, 223. b) H. G. von Schnering, H. Menke, *Z. Anorg. Allg. Chem.* **1976**, *424*, 108. c) R. Kröner, *Dissertation*, Universität Stuttgart, FRG, 1989. d) R. Kröner, R. Nesper, H. G. von Schnering, *Z. Kristallogr.* **1988**, *182*, 164. e) R. Kröner, R. Nesper, H. G. von Schnering, *Z. Kristallogr.* **1989**, *186*, 172. f) H. G. von Schnering, J. Curda, W. Carrillo-Cabrera, to be published. g) J. Llanos, *Dissertation*, Univ. Stuttgart, FRG, 1983. h) J. Llanos, R. Nesper, H. G. von Schnering, *Angew. Chem.* **1983**, *95*, 1026. *Angew. Chem. Int. Ed. Engl.* **1983**, *22*, 998.

[4] H. G. von Schnering, U. Bolle, J. Curda, K. Peters, W. Carrillo-Cabrera, M. Somer, M. Schultheiss, U. Wedig, *Angew. Chem.* **1996**, *108*, 1062. *Angew. Chem. Int. Ed. Engl.* **1996**, *35*, 984.

[5] H. Schäfer, *J. Solid State Chem.* **1985**, *57*, 97.

[6] R. Nesper, *Prog. Solid State Chem.* **1990**, *20*, 1.

[7] M. Atoji, *J. Chem. Phys.* **1961**, *35*, 1950.

[8] a) H. G. von Schnering, *Angew. Chem.* **1981**, *93*, 44. *Angew. Chem. Int. Ed. Engl.* **1981**, *20*, 33. b) H. G. von Schnering, W. Hönle in *Encyclopedia of Inorganic Chemistry*, R. Bruce King (Edit.), John Wiley & Sons, Ltd., London 1994, p. 3106.

[9] H. Bürger, R. Eujen, *Z. Anorg. Allg. Chem.* **1972**, *394*, 19.

[10] G. Kliche, H. G. von Schnering, *Z. Anorg. Allg. Chem.* **1992**, *608*, 131.

[11] G. Kliche, M. Schwarz, H. G. von Schnering, *Angew. Chem.* **1987**, *99*, 350; *Angew. Chem. Int. Ed. Engl.* **1987**, *26*, 349.

[12] J. Goubeau, *Advan. Chem. Ser.* **1964**, *42*, 87.

[13] J. Goubeau, O. Beurer, *Z. Anorg. Allg. Chem.* **1960**, *310*, 110.

[14] J. Goubeau, W. Anselment, *Z. Anorg. Allg. Chem.* **1960**, *310*, 248.

[15] M. Somer, *Chemiedozententagung*, Jena, Abstr. No. D7 (1995).